



Photometric Analysis for Asteroid (81) Terpsichore using Convex Inversion and Phase Function Fitting Methods

Ao Wang¹ , Xiaobin Wang^{2,3,4}, Xiaoyun Xu^{2,3,4}, Longhua Qin¹ , Quanguai Gao¹ , Huaizhen Li¹, Yong Xiao¹, and Hairu Zhao¹

¹Department of Physics, Yuxi Normal University, Yuxi 653100, China; wangao@yxnu.edu.cn

²Yunnan Observatories, Chinese Academy of Sciences, Kunming 650216, China

³Key Laboratory for the Structure and Evolution of Celestial Objects, Chinese Academy of Sciences, Kunming 650216, China

⁴University of Chinese Academy of Sciences, Beijing 100049, China

Received 2024 January 2; revised 2024 March 11; accepted 2024 March 26; published 2024 June 3

Abstract

The shapes and rotation states (periods and pole orientations) of main-belt asteroids are important for understanding their formation and evolution. In order to obtain sufficient photometric data covering different apparitions for asteroid (81) Terpsichore, ground-based photometric observations in 2020 and 2021 were carried out. By combining published and newly obtained photometric data, we calculated the shape and spin parameters for (81) Terpsichore using the convex inversion method. With this method, we have derived a best fitted pole orientation— $(22.2 \pm_{3.1}^{3.3}, 17.5 \pm_{5.5}^{10.8})$ with a spin period of $10.94 \pm_{0.01}^{0.01}$ h. Based on the derived convex shape of (81) Terpsichore, we have fitted the H , G_1 , G_2 phase function using the calibrated TESS data and Gaia data after accounting for the lightcurve amplitude correction. As a result, we have derived its absolute magnitude $H = 8.68 \pm_{0.19}^{0.22}$ mag with corresponding phase function parameters $G_1 = 0.82 \pm_{0.10}^{0.09}$ and $G_2 = 0.02 \pm_{0.02}^{0.03}$.

Key words: asteroids: general – minor planets – asteroids: individual (Terpsichore) – techniques: photometric

1. Introduction

Asteroids are a class of small celestial bodies in the solar system. They are thought to be valuable for studying the formation and evolution of the solar system because of their origin from the remnants of planetesimals from the early epoch of the solar system (Wang et al. 2019). Therefore, it makes scientific sense to study the spin orientation, rotation period, shape and other basic physical properties of asteroids to derive the information on the formation and evolution of both asteroids themselves and the solar system (Wang et al. 2015). There are only several asteroid targets (101955 Bennu (Lauretta et al. 2019), 162173 Ryugu (Watanabe et al. 2019), 4179 Toutatis (Huang et al. 2013) and so on) that have been imaged directly by spacecraft considering the cost and efficiency of exploration. For the majority of asteroids, ground-based observations, especially photometric observations, play a leading role in deriving their shapes, rotation periods, pole orientations and other basic physical parameters (Martikainen et al. 2021). From the time-resolved photometric observations, asteroids' lightcurves (variation of brightness over time) can be derived. Then, with the help of lightcurves obtained at several different apparitions, the shapes and spin parameters of asteroids can be derived (Kaasalainen & Torppa 2001; Kaasalainen et al. 2001). By the way, except for some slow rotators, most or sometimes the whole asteroids'

phased lightcurves can be obtained during one night's ground-based photometric observations (Pravec et al. 2002).

An asteroid phase curve refers to the variation of an asteroid's disk-integrated brightness over the phase angle, which is the angle between the directions to the observer and the Sun as seen from the asteroid (Wilawer et al. 2022). From an asteroid phase curve, we can (1) calculate the absolute magnitude H (apparent magnitude at 1 AU from both the Sun and the observer) and relate its value to the size and albedo of the asteroid; (2) probe the surface roughness, porosity, regolith and other surface properties of asteroids; and (3) derive a preliminary alternative for the taxonomic type of the asteroid before getting its spectral information (Penttilä et al. 2016; Shevchenko et al. 2016; Wilawer et al. 2022). For describing the asteroid phase curves, Bowell et al. (1989) developed the H , G phase function which was adopted by the International Astronomical Union (IAU) in 1985. Muinonen et al. (2010) proposed two new H , G_1 , G_2 and H , G_{12} functions and Penttilä et al. (2016) improved the H , G_{12} system. As a result, the inadequacies of the previous H , G phase function in estimating the absolute magnitude of an asteroid have been improved (Pál et al. 2020).

Traditionally, asteroid phase curves were derived from dense lightcurves obtained from ground-based observations. However, there are only a few hundred asteroids with high-quality phase curves and the increase in numbers is slow (Shevchenko

et al. 2016) because of the time-consuming feature of these ground-based observations. On the other hand, asteroid phase curves derived from sparse photometric data that are obtained by surveys like Gaia (Gaia Collaboration et al. 2023) and TESS (Pál et al. 2020) are often accompanied by relatively large uncertainties. This is mostly caused by not considering the lightcurve amplitude correction (Wilawer et al. 2022). Therefore, it makes sense to combine the determination of an asteroid phase function and lightcurve inversion of an asteroid. After deriving the rotation parameters and shape models (such as ellipsoid, Muinonen et al. 2015, and convex shape; Kaasalainen & Torppa 2001; Kaasalainen et al. 2001) of an asteroid from lightcurve inversion, the rotation brightness variation can be accounted for when determining the asteroid phase function using sparse photometry data.

(81) Terpsichore, as one target for applying the method mentioned above, was observed in 2020 and 2021 using the 1.0 m telescope at Yunnan Astronomical Observatory (YNAO) in China. Asteroid (81) Terpsichore is a C-type main-belt asteroid (Tholen & Barucci 1989) with a rotation period around 10.9 hr (Pilcher 2011; Franco et al. 2020; Pál et al. 2020). Considering that asteroid (81) Terpsichore is the core member of an asteroid dynamical family (Nesvorný 2015), the study of its rotation parameters, shape and phase function parameters mentioned above can give a valuable clue to the collisional evolution history of this asteroid family.

We are going to first obtain asteroid (81) Terpsichore's pole orientation and its corresponding convex shape by employing the convex inversion method (Kaasalainen & Torppa 2001; Kaasalainen et al. 2001). To do this, it is necessary to combine the newly obtained dense lightcurves (observed in 2020 and 2021 covering two different apparitions) and available published dense lightcurves. After that, based on the newly obtained convex shape and spin parameters, the phase function (Muinonen et al. 2010; Penttilä et al. 2016) can be fitted using calibrated TESS data (Pál et al. 2020) and sparse Gaia data (Gaia Collaboration et al. 2023).

This paper is organized as follows. In Section 2, the information on ground-based observations and data reduction for asteroid (81) Terpsichore is presented. Section 3 shows the procedure for the convex inversion method. The analysis of (81) Terpsichore's phase function is presented in Section 4. Finally, there is a summary in Section 5

2. Observation and Data Reduction

To obtain sufficient photometric data for (81) Terpsichore, we carried out photometric observations in 2020 and 2021 using the 1.0 m telescope at YNAO in China.⁵ All of the new photometric data were obtained through a clear filter.

⁵ <http://www.ynao.ac.cn/kyzz/omt/jj/>

As for the newly obtained CCD images, we performed the associated bias subtraction and flat correction according to the standard procedure using the Image Reduction and Analysis Facility⁶ (IRAF) software. The occasional cosmic rays on the images were identified by a criterion of five times the standard deviation of sky background and then removed. With the help of the APPHOT package in IRAF, we measured the instrumental magnitudes of reference stars and the asteroid target. To do this, we used apertures with 2 times full width at half maximum (FWHM) of stars' point-spread function as the optimal aperture.

We also downloaded the available published data on (81) Terpsichore from the Asteroid Lightcurve Photometry Database (ALCDEF) website.⁷ Table 1 shows information on the photometric observations of asteroid (81) Terpsichore.

Before the determination of spin parameters and the convex shape of (81) Terpsichore, it is necessary to compute the light-time corrected Julian Date (JD) epoch and calculate the ecliptic asteroid-centric Cartesian coordinates of the Sun and observers in astronomical units (Durech et al. 2009, 2010). To do this, we used the Ephemeris Service provided by the Minor Planet Center⁸ to calculate the equatorial asteroid-centric Cartesian coordinates of the Sun and observers in astronomical units.

3. Determination of Spin Parameters and Convex Shape

The lightcurve inversion of asteroids provides us with a way to understand asteroids' physical properties such as rotation periods, pole orientations and shapes. To derive the convex shape and spin parameters of (81) Terpsichore from the photometric data, we used the convex inversion method (Kaasalainen et al. 2001; Kaasalainen & Torppa 2001; Kaasalainen et al. 2002). This method is based on the optimization of unknown parameters of the shape (modeled as a convex hull), rotation period, pole orientation and the scattering law. The source codes of the convex lightcurve inversion routines together with brief manuals are available on the DAMIT (Durech et al. 2009, 2010) web page.⁹

In order to carry out the convex lightcurve inversion for (81) Terpsichore, we combined available existing data (the ground-based dense photometric data of Pilcher (2010, 2011) and data from space observations by TESS (Pál et al. 2020)) with our newly obtained data observed in 2020 and 2021. In all, 36 dense lightcurves in five different apparitions are involved in our analysis. Figure 4 shows some of the available lightcurves,¹⁰ including observed data and modeled ones.

⁶ IRAF is distributed by the National Optical Astronomy Observatories, which are operated by the Association of Universities for Research in Astronomy, Inc., under cooperative agreement with the National Science Foundation.

⁷ <https://alcdef.org/index.php>

⁸ <https://minorplanetcenter.net/iau/MPEph/MPEph.html>

⁹ http://astro.troja.mff.cuni.cz/projects/asteroids3D/web.php?page=project_main_page

¹⁰ Covering more than 60% of the rotation period.

Table 1
Information on the Photometric Observations of Asteroid (81) Terpsichore

Date (UT)	Δ (au)	r (au)	α ($^\circ$)	V -mag	Filter	Observers/Telescope
2009-10-24.3	1.371	2.265	14.2	11.9	<i>R</i>	Pilcher (2010) Figure 4(e)
2009-10-26.4	1.359	2.264	13.4	11.9	<i>R</i>	Pilcher (2010) Figure 4(h)
2009-10-28.3	1.348	2.264	12.6	11.9	<i>R</i>	Pilcher (2010) Figure 4(k)
2009-11-07.2	1.307	2.265	8.6	11.6	<i>R</i>	Pilcher (2010)
2009-11-10.3	1.300	2.265	7.4	11.6	<i>R</i>	Pilcher (2010) Figure 4(k)
2009-11-23.2	1.292	2.267	5.2	11.4	<i>R</i>	Pilcher (2010)
2009-12-05.2	1.324	2.272	8.9	11.7	<i>R</i>	Pilcher (2010)
2011-02-15.4	2.181	3.036	11.0	13.5	<i>C</i>	Pilcher (2011)
2011-02-17.4	2.168	3.040	10.4	13.4	<i>C</i>	Pilcher (2011)
2011-02-26.4	2.122	3.057	7.3	13.3	<i>C</i>	Pilcher (2011) Figure 4(a)
2011-03-14.2	2.093	3.085	1.3	12.9	<i>C</i>	Pilcher (2011)
2011-03-15.3	2.094	3.087	0.9	12.9	<i>C</i>	Pilcher (2011) Figure 4(b)
2018-08-04.3	1.754	2.739	6.5	12.6	<i>GR</i>	Pál (2020) Figure 4(c)
2018-08-05.1	1.751	2.737	6.2	12.6	<i>GR</i>	Pál (2020)
2018-08-06.1	1.745	2.735	5.9	12.5	<i>GR</i>	Pál (2020)
2018-08-07.1	1.740	2.733	5.5	12.5	<i>GR</i>	Pál (2020)
2018-08-07.8	1.737	2.731	5.2	12.5	<i>GR</i>	Pál (2020) Figure 4(d)
2018-08-09.3	1.729	2.728	4.7	12.5	<i>GR</i>	Pál (2020)
2018-08-10.1	1.726	2.726	4.5	12.4	<i>GR</i>	Pál (2020)
2018-08-11.1	1.722	2.724	4.1	12.4	<i>GR</i>	Pál (2020)f
2018-08-12.1	1.719	2.722	3.8	12.4	<i>GR</i>	Pál (2020)
2018-08-13.1	1.715	2.720	3.5	12.4	<i>GR</i>	Pál (2020) Figure 4(g)
2018-08-14.1	1.712	2.717	3.3	12.3	<i>GR</i>	Pál (2020)
2018-08-15.1	1.709	2.715	3.1	12.3	<i>GR</i>	Pál (2020)
2018-08-16.1	1.706	2.713	2.9	12.3	<i>GR</i>	Pál (2020)
2018-08-17.1	1.704	2.711	2.8	12.3	<i>GR</i>	Pál (2020)
2018-08-18.1	1.702	2.709	2.8	12.3	<i>GR</i>	Pál (2020)
2018-08-19.1	1.700	2.706	2.8	12.3	<i>GR</i>	Pál (2020)
2018-08-20.1	1.698	2.704	2.9	12.3	<i>GR</i>	Pál (2020)
2018-08-21.1	1.697	2.702	3.0	12.3	<i>GR</i>	Pál (2020)
2018-08-22.1	1.696	2.700	3.2	12.3	<i>GR</i>	Pál (2020)
2018-08-22.6	1.695	2.699	3.4	12.3	<i>GR</i>	Pál (2020)
2020-02-12.5	1.666	2.526	13.6	12.6	<i>C</i>	1.0 m, YNAOi
2020-02-13.5	1.675	2.528	13.9	12.6	<i>C</i>	1.0 m, YNAOj
2021-05-08.5	2.459	3.351	9.4	13.9	<i>C</i>	1.0 m, YNAO
2021-05-09.5	2.468	3.352	9.7	13.9	<i>C</i>	1.0 m, YNAO

Note. Δ and r are the geocentric and heliocentric distance of the asteroid respectively. α means the phase angle of the object and V -mag is the predicted visual magnitude.

According to the manual, since we used relative lightcurves obtained by ground-based observations, the parameters of the scattering law were fixed as $a=0.5$, $d=0.1$ and $k=-0.5$ (where a is the amplitude and d is the scale length of the opposition effect, and k is the overall slope of the phase curve, Kaasalainen et al. 2003). We fixed the Lambert's coefficient to $c=0.1$ because it usually has only a minor effect on the inversion solution.

After setting the parameters of the scattering law, we moved on to a very important step on our way to getting a convex model—finding the *correct* rotation period of the asteroid. We scanned the period interval from 4.0 to 20.0 hr (typical rotation period range for an asteroid) with a step of $P^2/2\Delta T$ (see

Figure 1) where ΔT is the time span of the photometric data involved in our inversion. It is based on the fact that the maxima and minima of a double-sinusoidal lightcurve for periods P and $P \pm \Delta P$ are at the same epochs after ΔT time (Durech et al. 2010).

During the procedure of each period scanning step in the inversion, six initial poles were tested. According to Durech et al. (2010), the rotation parameters and coefficients of a truncated spherical harmonic series (degree l and order m of a Laplace series expansion, usually up to 8) were derived by the Levenberg–Marquardt algorithm. Then we found that the most significant minimum of root mean square (rms) was around 10.94 hr (see Figure 1). Based on this best fitted rotation period,

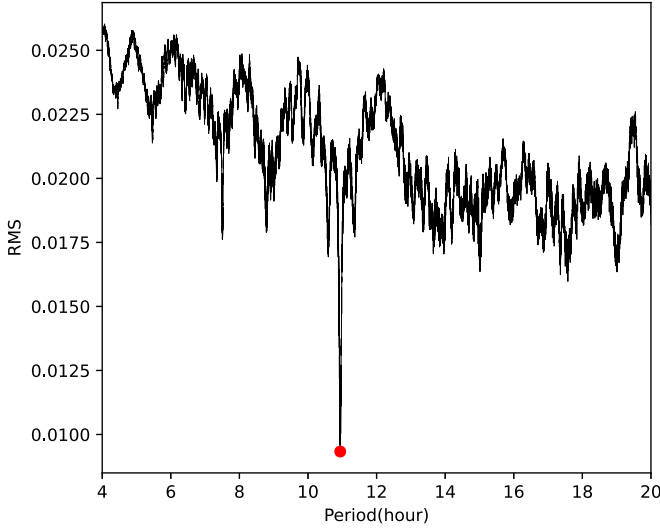


Figure 1. Period distributions of (81) Terpsichore vs. rms. Red dot is the minimum of rms, about 0.009 (corresponding period is about 10.94 hr).

we ran the convexinv procedure¹¹ with different fixed initial poles (using one-degree meshes over the unit spherical surface) to search for the best-fitting rotation pole orientation.

We found that the minimum of rms was around $(24^\circ, 33^\circ)$. Based on this initial value of pole orientation, we then optimized the pole solution by setting the pole longitude and latitude as free parameters during the convexinv procedure and finally obtained the best fitted pole orientation $(22.2^\circ, 17.5^\circ)$. The contours of rms versus the trial poles are displayed in Figure 2.

Considering that the convex inversion method seeks to adjust free parameters in order to minimize a χ^2 -type target function,¹² we chose solutions with a 6.5% larger χ^2 value (corresponding to a 3.2% larger rms value) than the global minimum as still admissible solutions (Vokrouhlický et al. 2011). Because in our case the total number of observations $N \approx 4300$ and the number of parameters $M \approx 100$, the number of degrees of freedom is $\nu = N - M \approx 4200$ and the 6.5% increase of χ^2 corresponds to about a 3σ interval of the χ^2 distribution with ν degrees of freedom.¹³

Based on the distributions of admissible solutions with a 3.2% larger rms value than the global minimum mentioned above, we calculated the 3σ boundary for each distribution. Then we estimated the uncertainties of rotation parameters

using the intervals between the best fitted solution and the 1σ limits for each distribution. In this way, we obtained $10.94 \pm_{0.01}^{0.01}$ hr as the best fitted rotation period and $(22.2 \pm_{3.1}^{3.3}, 17.5 \pm_{5.5}^{10.8})$ as the best fitted pole orientation with corresponding uncertainties. By the way, for one asteroid, there are usually two pole solutions with about a 180 degree difference in longitude during the lightcurve inversion due to a limited geometry (an asteroid orbiting too close to the ecliptic, see Kaasalainen & Lamberg 2006 for details). The mirror pole solution was not adopted here because its 3σ boundary of the χ^2 distribution would be cut off by a region with χ^2 values larger than 3σ .

After rotation parameters were obtained, we could deal with the convex shape of (81) Terpsichore. The 3D convex shape of (81) Terpsichore was constructed based on the spherical-harmonic series obtained with the help of the Minkowski procedure (Durech et al. 2010). According to the manual of the conjgradinv procedure (Durech et al. 2010), we optimized the shape of (81) Terpsichore with rotation and scattering parameters fixed, and the derived convex shape is illustrated in Figure 3.

4. Phase Function Analysis

The photometric phase curve of an asteroid means the magnitude as a function of the phase angle. Its shape can provide us with information on the taxonomic type of the asteroid before the corresponding spectral information is available (Oszkiewicz et al. 2012; Penttilä et al. 2016; Shevchenko et al. 2016). In 1989, the $H - G$ phase function was adopted as the standard photometric system for asteroids by the IAU (Bowell et al. 1989). The $H - G_1 - G_2$ and H, G_{12} phase function proposed by Muinonen et al. (2010) was adopted as a new photometric system by IAU in 2012. The new phase function behaves better in the back scattering effect for high- and low-albedo asteroids than before.

Here, we joined the data of Gaia (phase angle $\alpha > 10^\circ$) (Gaia Collaboration et al. 2023) and data obtained from TESS ($\alpha < 10^\circ$) (Szabó et al. 2022) to determine the $H - G_1 - G_2$ parameters of asteroid (81) Terpsichore. The Gaia G -band observation data were obtained from the Gaia Archive website¹⁴ and converted to the Johnson V -band magnitude system using the following relationship (Gaia Collaboration et al. 2023)

$$\begin{aligned} G - V &= -0.04749 - 0.0124 * (B - V) - 0.2901 * (B - V)^2 \\ &\quad + 0.02008 * (B - V)^3 + 0.04772 * (B - V)^4. \end{aligned} \quad (1)$$

¹¹ According to descriptions on https://astro.troja.mff.cuni.cz/projects/damit/pages/software_download.

¹² $\chi^2 = (\sum_{i=1}^N (O - C)_i^2 / \sigma_i^2) / (N - M)$, where N is the total number of observations and M is the number of solved parameters of the model, σ_i is their estimated uncertainty, and the $(O - C)_i$ is the difference between the observed and computed brightnesses.

¹³ The χ^2 distribution with ν degrees of freedom has a mean of ν and a variance of 2ν (Press et al. 2007).

¹⁴ <https://gea.esac.esa.int/archive/>

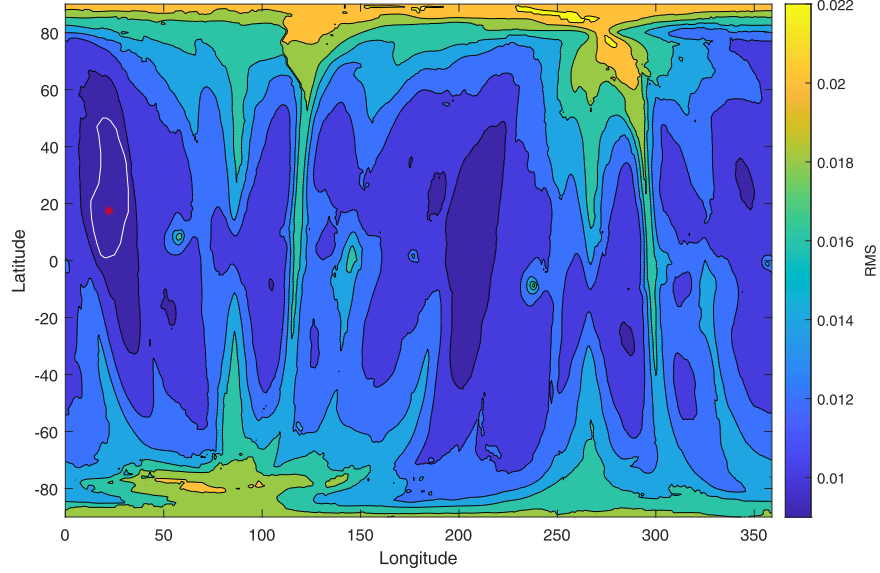


Figure 2. Pole distributions of (81) Terpsichore vs. rms. Red asterisk is the best fitted pole orientation (22° , 17.5°) with rms about 0.009. White line is the boundary of admissible pole solutions (6.5% larger χ^2 value, 3.2% larger rms value than the corresponding global minimum).



Figure 3. Convex shape of (81) Terpsichore. The projected shapes viewed along the X , Y and Z -axes are drawn from left to right respectively.

There are 26 sparse data points in all covering the phase angle α from 13.1° to 26.5° . As for the $B - V$ color index, we got its value of 0.701 for (81) Terpsichore from the UBV Mean Asteroid Colors (Tedesco 2005). The TESS G_{RP} band observation data were downloaded from the ALCDEF website¹⁵ (The TESS data in ALCDEF have been split into individual lightcurves, see Table 1) and converted to the Johnson V -band magnitude system using the following relationship

$$G_{RP} - V = 0.01868 - 0.9028 * (V - I_C) - 0.005321 * (V - I_C)^2 - 0.004186 * (V - I_C)^3. \quad (2)$$

As for the $V - I_C$ color index, we computed its value for (81) Terpsichore based on the $G - V$ color index obtained

above using the following relationship (Gaia Collaboration et al. 2023)

$$\begin{aligned} G - V &= -0.01597 - 0.02809 * (V - I_C) - 0.2483 * (V - I_C)^2 \\ &\quad + 0.03656 * (V - I_C)^3 - 0.002939 * (V - I_C)^4. \end{aligned} \quad (3)$$

After that, we accounted for the effects on magnitude due to the varying distance of the asteroid from the Sun and the observer by the formula $-5 \log(r\Delta)$ (r is the distance from the Sun to the asteroid and Δ is the distance from the observer to the asteroid (in astronomical units)), because the brightness is standardized by fictitiously locating the asteroid at a 1 AU distance from the Sun as well as from the observer.

¹⁵ <https://alcdef.org/index.php>

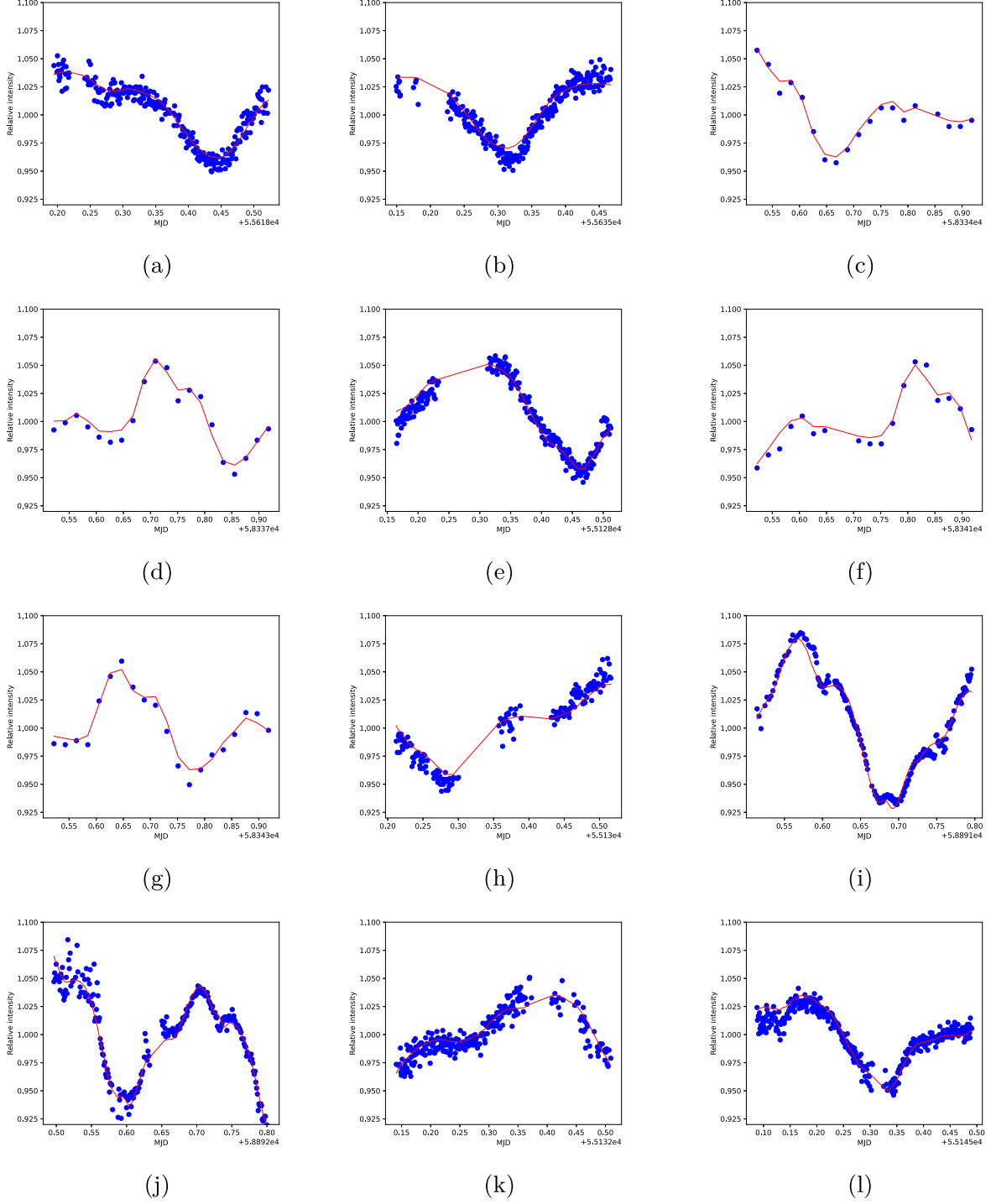


Figure 4. Lightcurves of (81) Terpsichore. Blue dot symbols are observed data, and red solid lines are modeled using the convex shape model.

For determination of the $H - G_1 - G_2$ phase function parameters, we utilized the average magnitude over a whole rotation period corresponding to each sparse data point. To do this, we computed theoretically modeled intensity based on the derived convex shape and rotation parameters. For each sparse

calibrated photometric data point, we computed the individual magnitude correction ΔM_i using the following equation and subtracted it from the original photometric data.

$$\Delta M_i = -2.5 \lg(I_i/I_a), \quad (4)$$

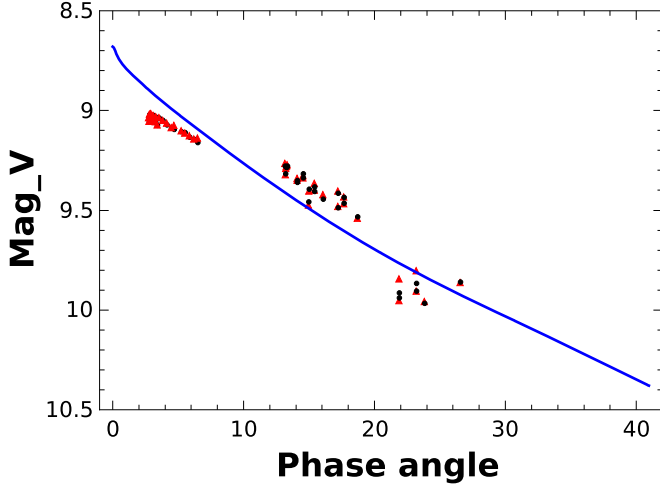


Figure 5. Photometric phase curve of (81) Terpsichore (blue line) combining the data from Gaia (phase angle $\alpha > 10^\circ$) and data obtained from TESS ($\alpha < 10^\circ$). Black dots are raw observed data, and red dots are data with rotation effects removed.

where I_i is the i th theoretically modeled intensity assuming the derived convex shape and rotation parameters of (81) Terpsichore, and I_a is the corresponding average intensity over a whole rotation period.

In the next step, we considered fitting the $H - G_1 - G_2$ phase function in magnitude form as follows

$$V(\alpha) = H - 2.5 \log_{10}[G_1 \Phi_1(\alpha) + G_2 \Phi_2(\alpha) + (1 - G_1 - G_2) \Phi_3(\alpha)], \quad (5)$$

where $\Phi_1(\alpha)$, $\Phi_2(\alpha)$ and $\Phi_3(\alpha)$ are three basis functions. The basis functions include linear parts, a constant part and parts defined by cubic splines (see Muinonen et al. 2010; Penttilä et al. 2016 for more details).

With the help of the HG1G2 tools,¹⁶ the $H - G_1 - G_2$ phase function was fitted for (81) Terpsichore using the linear least-squares method (Penttilä et al. 2016). We estimated its absolute magnitude $H = 8.68 \pm_{0.19}^{0.22}$ mag with two phase function parameters $G_1 = 0.82 \pm_{0.10}^{0.09}$ and $G_2 = 0.02 \pm_{0.02}^{0.03}$. The uncertainties based on 1σ limits of distributions were given by the Fortran 2003 version of the HG1G2 tools. As a result, the corresponding photometric phase curve is presented as a line in Figure 5. The H value obtained by us is close to the IAU-adopted absolute V magnitude ($H = 8.48$) (Tholen 2009) and the values of two phase function parameters G_1 , G_2 support that asteroid (81) Terpsichore is a C-type asteroid according to Oszkiewicz et al. (2012).

Given these phase function parameters, the phase integral parameter q , normalized slope of the phase-curve k and the amplitude of opposition effect $\zeta - 1$ (ζ is the enhancement

factor) were estimated to be 0.36, -1.88 and 0.19 respectively using the following relationships (Muinonen et al. 2010):

$$\begin{aligned} q &= 0.009082 + 0.4061G_1 + 0.8092G_2, \\ k &= -\frac{1}{5\pi} \frac{30G_1 + 9G_2}{G_1 + G_2} \\ \zeta - 1 &= \frac{1 - G_1 - G_2}{G_1 + G_2}. \end{aligned} \quad (6)$$

Based on the derived absolute magnitude H and the relationship of diameter and albedo ($D = \frac{1329}{\sqrt{p_v}} 10^{-0.2H}$) (Bowell et al. 1989), the equivalent diameter D of (81) Terpsichore was estimated to be about 109 km using the albedo of 0.05 (Davis & Neese 2005), which is slightly smaller than the previous value about 120 km (Tedesco et al. 2004; Mainzer et al. 2016).

5. Summary

In order to study the physical properties of asteroid (81) Terpsichore, we carried out four nights of photometric observations in 2020 and 2021 using the 1.0 m telescope at YNAO in China. Combining our four newly obtained lightcurves (covering two different apparitions) with 32 lightcurves from the MPC ALCDEF database (mainly from TESS, Pál et al. 2020, covering three different apparitions), the shape and spin parameters of (81) Terpsichore have been analyzed by us with the convex inversion method (Kaasalainen et al. 2001). The best rotation period of $10.94 \pm_{0.01}^{0.01}$ hr obtained by us is consistent with previous results (10.945 hr by Pilcher 2011, 10.946 hr by Franco et al. 2020 and 10.939 hr by Pál et al. 2020). Then we first derived the rotation pole orientation of (81) Terpsichore—($22.2 \pm_{3.1}^{3.3}^\circ$, $17.5 \pm_{5.5}^{10.8}^\circ$) and its corresponding convex shape model (see Figure 3).

After that, we joined the sparse data of Gaia (Gaia Collaboration et al. 2023) and data obtained by TESS (Szabó et al. 2022) to determine the $H - G_1 - G_2$ parameters of asteroid (81) Terpsichore by converting these data into the Johnson V -band magnitude system. We considered that the variations caused by the shape effect could have an influence on the fitted H value of the phase function when using observation data obtained at different epochs. Our main idea to deal with these variations is to use the average magnitude over a whole rotation period corresponding to each sparse data point to determine the $H - G_1 - G_2$ parameters. This correction is more significant in Gaia sparse data (see Figure 5). Then, the $H - G_1 - G_2$ phase function was fitted and we adopt the result $H = 8.68 \pm_{0.19}^{0.22}$, $G_1 = 0.82 \pm_{0.10}^{0.09}$ and $G_2 = 0.02 \pm_{0.02}^{0.03}$. This absolute V magnitude H is close to the previous IAU-adopted value ($H = 8.48$). The values of G_1 , G_2 parameters support that asteroid (81) Terpsichore is a C-type asteroid which is consistent with the previous result of asteroid taxonomy by Neese (2010).




¹⁶ <https://wiki.helsinki.fi/display/PSR/HG1G2+tools>

Our research provides a scheme for taking advantage of calibrated sparse data together with dense photometric data. On the one hand, dense photometric data mainly obtained by ground-based telescopes are suitable for determining shapes and rotation parameters of asteroids. On the other hand, calibrated sparse data like TESS data (Szabó et al. 2022) and Gaia data (Gaia Collaboration et al. 2023) are very useful for fitting the phase function of asteroids.

Acknowledgments

The authors would like to thank the anonymous referee for the helpful comments. The authors acknowledge the financial support from the Science Research Foundation of Yunnan Education Department of China (grant 2020J0649) and the Natural Science Foundation of Yunnan Province (grant 202101AU070010). The authors acknowledge the computing support provided by the JRT Science Data Center at Yuxi Normal University. Ao Wang acknowledges the financial support from the Hundred Talents Program of Yuxi (grant 2019-003).

ORCID iDs

Ao Wang  <https://orcid.org/0000-0002-0005-5218>
 Longhua Qin  <https://orcid.org/0000-0001-7905-4295>
 Quanguai Gao  <https://orcid.org/0000-0001-9732-069X>

References

- Bowell, E., Hapke, B., Domingue, D., et al. 1989, in Asteroids II, ed. R. P. Binzel, T. Gehrels, & M. S. Matthews (Tucson, AZ: Univ. Arizona Press), 524
- Davis, D. R., & Neese, C. 2005, PDSS, 26, 1
- Durech, J., Kaasalainen, M., Warner, B. D., et al. 2009, *A&A*, 493, 291
- Durech, J., Sidorin, V., & Kaasalainen, M. 2010, *A&A*, 513, A46
- Franco, L., Marchini, A., Saya, L.-F., et al. 2020, MPBu, 47, 242
- Gaia Collaboration, Vallenari, A., & Brown, A. G. A. 2023, *A&A*, 674, A1
- Huang, J., Ji, J., Ye, P., et al. 2013, *NatSR*, 3, 3411
- Kaasalainen, M., & Lamberg, L. 2006, *InvPr*, 22, 749
- Kaasalainen, M., Mottola, S., & Fulchignoni, M. 2002, in Asteroids III, ed. W. F. Bottke, Jr., A. Cellino, P. Paolicchi, & R. P. Binzel (Tucson, AZ: Univ. Arizona Press), 139
- Kaasalainen, M., & Torppa, J. 2001, *Icar*, 153, 24
- Kaasalainen, M., Torppa, J., & Muinonen, K. 2001, *Icar*, 153, 37
- Kaasalainen, S., Piironen, J., Kaasalainen, M., et al. 2003, *Icar*, 161, 34
- Lauretta, D. S., Dellagiustina, D. N., Bennett, C. A., et al. 2019, *Natur*, 568, 55
- Mainzer, A. K., Bauer, J. M., Cutri, R. M., et al. 2016, PDSS., 247, 1
- Martikainen, J., Muinonen, K., Penttilä, A., Cellino, A., & Wang, X. B. 2021, *A&A*, 649, A98
- Muinonen, K., Belskaya, I. N., Cellino, A., et al. 2010, *Icar*, 209, 542
- Muinonen, K., Wilkman, O., Cellino, A., Wang, X., & Wang, Y. 2015, *P&SS*, 118, 227
- Neese, C. 2010, PDSS, 123, 1
- Nesvorný, D. 2015, PDSS, 234, 1
- Oszkiewicz, D. A., Bowell, E., Wasserman, L. H., et al. 2012, *Icar*, 219, 283
- Pál, A., Szakáts, R., Kiss, C., et al. 2020, *ApJS*, 247, 26
- Penttilä, A., Shevchenko, V. G., Wilkman, O., & Muinonen, K. 2016, *P&SS*, 123, 117
- Pilcher, F. 2010, MPBu, 37, 45
- Pilcher, F. 2011, MPBu, 38, 156
- Pravec, P., Harris, A. W., & Michalowski, T. 2002, Asteroids III, 113
- Press, W. H., Teukolsky, S. A., Vetterling, W. T., & Flannery, B. P. 2007, Numerical Recipes. The Art of Scientific Computing (3rd ed.; Cambridge: Cambridge Univ. Press)
- Shevchenko, V. G., Belskaya, I. N., Muinonen, K., et al. 2016, *P&SS*, 123, 101
- Szabó, G. M., Pál, A., Szigeti, L., et al. 2022, *A&A*, 661, A48
- Tedesco, E. F. 2005, PDSS, 30, 1
- Tedesco, E. F., Noah, P. V., Noah, M., & Price, S. D. 2004, PDSS, 12, 1
- Tholen, D. J. 2009, PDSS, 105, 1
- Tholen, D. J., & Barucci, M. A. 1989, in Asteroids II, ed. R. P. Binzel, T. Gehrels, & M. S. Matthews (Tucson, AZ: Univ. Arizona Press), 298
- Vokrouhlický, D., Durech, J., Polishook, D., et al. 2011, *AJ*, 142, 159
- Wang, A., Wang, X., Muinonen, K., & Han, X. L. 2019, *P&SS*, 167, 17
- Wang, X., Muinonen, K., Wang, Y., et al. 2015, *A&A*, 581, A55
- Watanabe, S., Hirabayashi, M., Hirata, N., et al. 2019, *Sci*, 364, 268
- Wilawer, E., Oszkiewicz, D., Kryszyńska, A., et al. 2022, *MNRAS*, 513, 3242